Anal. Bioanal. Electrochem., Vol. 15, No. 2, 2023, 137-149
https://www.doi.org/10.22034/abec.2023.702331

Analytical & Bioanalytical Electrochemistry

Full Paper

Irreversible Inactivation of Initial Form of Water-Soluble Redox Proteins-Theoretical Study in Square-Wave Voltammetry

Pavle Apostoloski, and Rubin Gulaboski*

Faculty of Medical Sciences, "Goce Delcev" University Stip, Republic of Macedonia

*Corresponding Author, Tel.: +38975331078
E-Mail: rubin.gulaboski@ugd.edu.mk

Received: 6 January 2023 / Received in revised form: 17 February 2023 / Accepted: 18 February 2023 / Published online: 28 February 2023

Abstract- Inactivation of water-soluble redox proteins and enzymes is often encountered in many biological systems under physiological conditions. In electrochemical experiments, if the initial redox form of a given water-soluble redox protein is engaged at the same time in an electrochemical transformation on the working electrode and in an irreversible chemical reaction, then the voltammetric outputs might show quite specific behavior due to the simultaneous interplay of electron transfer step and the chemical reaction. In this work, we present for the first time theoretical results of such a model applicable to the electrochemistry of hydrophilic redox proteins under conditions of square-wave voltammetry. We present the readers a large tabular overview of a series of voltammetric patterns of this electrode mechanism calculated at different rates of electron transfer step and different kinetics of chemical step. Moreover, in the work we give hints to apply suitable methodology to recognize this mechanism under conditions of square-wave voltammetry, while giving directions on how to assess the kinetics of both steps involved in this mechanism. The results elaborated in this work should be of help to experimentalists working in enzymatic voltammetry.

Keywords- Electrochemistry of enzymes; Kinetics of enzyme inactivation; Square-wave voltammetry; Theoretical modeling; Enzymatic voltammetry

1. INTRODUCTION

Redox enzymes play significant role in crucial physiological processes such as energy creation, protein synthesis and in transfer of physiologically important systems across cell membranes. Since enzyme inactivation is a common event taking place in physiological conditions, significant efforts in pharmacology and biochemistry have been focused on establishing experimental protocols to get insight into the mechanism of inactivation of various redox proteins and enzymes [1,2]. Very often, with strategically designed in-vitro experiments, one gets important information related to the activity of redox proteins and enzymes of interest [1]. Moreover, such studies coupled with theoretical molecular-dynamic simulations provide valuable platform in getting hints about reactivity of defined groups in proteins structure [3]. For taking deeper insight into mechanism of inactivation of redox proteins, electrochemistry is commonly a preferable instrumental tool. Since cyclic voltammetry can provide clues about mechanism of redox activity of many lipid-soluble and water-soluble proteins, this technique has been recognized as a major electrochemical tool that is quite suitable for studying redox activity of many enzymes [4-11]. Over the past two decades, square-wave voltammetry (SWV) has gained recognition as a dependable voltammetric method for investigating various aspects concerning the functionality of significant enzymatic and non-enzymatic systems [12-16]. Indeed, the theoretical modeling of electrode mechanisms in SWV is seen as an inevitable step to establish diagnostic criteria about mechanism going on in electrochemical transformation of defined redox proteins. Although there are many theoretical models relevant to describe various aspects of redox proteins in SWV [10,12,15,16], so far there is no theoretical work that reports on electrode mechanism where the starting redox form of defined water-soluble protein is involved in the same time in electrochemical transformation at the working electrode and in an irreversible chemical reaction. Elaborating on the theoretical aspects of such an electrode mechanism could prove to be extremely valuable, as it may provide insights into the inactivation mechanism of numerous water-soluble redox proteins. This study presents the outcomes of a theoretical SWV model, which considers an electrode transformation of a hydrophilic redox protein whose initial redox form is simultaneously participating in an irreversible chemical reaction. The findings presented in this work should prove beneficial for experimentalists working in enzymatic voltammetry, enabling them to identify this particular electrochemical mechanism and devise appropriate approaches to ascertain kinetic parameters essential for describing enzyme activity.

2. MATHEMATICAL MODEL

The mathematical model under consideration involves an electrochemical mechanism of electrochemically active species that are fully water-soluble. The initial redox form of these species, denoted as "Ox", undergoes simultaneous transformation on the working electrode and in irreversible chemical reaction (Scheme I):

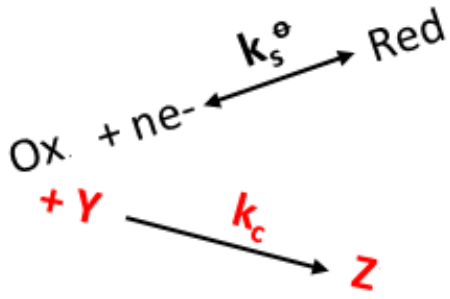

(I)

Scheme I. Schematic description of the model elaborated in this work

We assume in the model that the molecules of all species Ox, Red and Z are completely soluble in water and there are no adsorption phenomena taking place in the system. Ox and Red are oxidized and reduced form of a given water-soluble redox protein/enzyme, respectively. We suppose in the model that the transfer of mass of electrochemically active species "Ox" and "Red" to and from electrode surface takes place via semi-infinitive planar diffusion. Symbol "Y" stays to designate a substrate that selectively reacts in a chemically irreversible manner with Ox species in reaction scheme (I). It is also assumed that both, the molecules of "Y" and those of chemically created "Z" species, show no electrochemical activity in the range of applied potentials.

Mathematically, the considered mechanism can be described by following equations:

$$(\delta c(\mathrm{Ox})/\mathrm{d}t) = D[\delta^2 c(\mathrm{Ox})/\mathrm{d}x^2] - k_c c(\mathrm{Ox}) \quad (1)$$

$$(\delta c(\mathrm{Red})/\mathrm{d}t) = D[\delta^2 c(\mathrm{Red})/\mathrm{d}x^2] \quad (2)$$

$$(\delta c(\mathrm{Z})/\mathrm{d}t) = D[\delta^2 c(\mathrm{Z})/\mathrm{d}x^2] + k_c c(\mathrm{Ox}) \quad (3)$$

The differential equations (1-3) have been solved under following conditions:

$$t = 0;\ c(\mathrm{Ox}) = c^*(\mathrm{Ox});\ c(\mathrm{Red}) = c(\mathrm{Z}) = 0 \quad (4)$$

$$t > 0;\ x \rightarrow \infty;\ c(\mathrm{Ox}) \rightarrow c^*(\mathrm{Ox});\ c(\mathrm{Red}) + c(\mathrm{Z}) \rightarrow 0 \quad (5)$$

$$t > 0,\ x = 0; \quad (6)$$

$$(\delta c(\mathrm{Ox})/\mathrm{d}x) = I/(nFDS) \quad (7)$$

$$(\delta c(\mathrm{Red})/\mathrm{d}x) = -I/(nFDS) \quad (8)$$

$$D(\delta c(\mathrm{Z})/\mathrm{d}x) = 0 \quad (9)$$

At the surface of working electrode, the Butler-Volmer formalism applies in following form

$$(I/nFS) = k_s^\ominus \exp(-\alpha\Phi)\,[c(\mathrm{Ox}) - \exp(\Phi)\,c(\mathrm{Red})] \quad (10)$$

A well-known method of Nicholson and Olmstead reported in [17] has been explored to get numerical solution of equation (10) solved under conditions (1)-(9). An original

MATHCAD working file containing all recurrent formulas and the parameters used to calculate theoretical voltammograms of this model is given in the Supplementary Material.

Table 1. Definitions of all parameters used in calculating the square-wave voltammograms of electrode mechanism considered in this work

Symbol of Physical Parameter/Units	**Meaning of the Parameter**	**Definition**
Ψ	Dimensionless current	$\Psi = I/[(nFSc^*(\mathrm{Ox})(fD)^{1/2}]$
I/A	Electric current	
n	Number of exchanged electrons	1
S /cm^2	Surface area of working electrode	
x/cm	Distance to the working electrode surface	
F/ C mol^{-1}	Faraday constant	96485 C mol^{-1}
T/K	Thermodynamic temperature	298 K
t_p/s	duration of a single potential pulse in SWV	
f/Hz	Square-wave frequency	$f = t_p/2$
$c^*(\mathrm{Ox})$/mol cm^{-3}	Initial molar concentration of redox species Ox	
c(Ox), c(Red) and c(Z)/mol cm^{-3}	Molar concentrations of species Ox, Red, and Z, respectively	
c(Y)/mol cm^{-3}	Molar concentration of substrate Y	
α	Electron transfer coefficient	0.5
R/J mol^{-1}K^{-1}	Universal gas constant	8.314 J mol^{-1}K^{-1}
Φ	Dimensionless potential	$\Phi = \frac{nF}{RT}\left(E - E^{\phi'}\right)$
E / V	Applied potential	
$E^{\theta'}$/ V	Formal redox potential of couple Ox/Red	0.00 V
K_{ET}	Dimensionless parameter related to electron transfer step	$K_{ET} = k_s^{\theta}/(fD)^{1/2}$
k_s^{θ} / cm s^{-1}	Standard rate constant of electron transfer step	
D/ cm^2 s^{-1}	Diffusion coefficient	0.000005 cm^2 s^{-1}
K_{chem}	Dimensionless parameter related to rate of irreversible chemical reaction	$K_{chem} = k_c/f$
k_c / s^{-1}	Rate constant of irreversible chemical reaction	$k_c = k_c' \times c$(Y)
k_c'/mol^{-1} cm^3 s^{-1}	Real rate constant of irreversible chemical reaction	
E_{sw} / mV	Square-wave amplitude	50 mV
dE / mV	Potential step	4 mV
M	Numerical integration factor	$M = \mathrm{erfc}[K_{chem}(m/50)]^{1/2} - \mathrm{erfc}[K_{chem}(m\text{-}1)/50]^{1/2}$
m	Serial number of the time intervals	

When the instrumental parameters and temperature remain constant, the characteristics of the computed voltammetric results are primarily influenced by two dimensionless parameters: K_{ET} and K_{chem}. The dimensionless kinetic parameter K_{ET} is related to electron transfer step, and it is defined as $K_{ET} = k_s^{e}/(Df)^{0.5}$. The magnitude K_{ET} is indicative of the electron transfer kinetics between the working electrode and the redox species Ox and Red, in relation to the rate of diffusion of electrochemically active species and the pulse duration applied in SWV. On the other side, the value of dimensionless chemical kinetic parameter K_{chem} (defined as $K_{chem} = k_c/f$) portrays the rate of irreversible chemical reaction relative to the time duration of SW pulses. For the mechanism considered in this work, the rate constant k_c in last equation can be defined as: $k_c = k_c' \times c(Y)$, where k_c' stays for the real chemical rate constant, while $c(Y)$ is molar concentration of substrate "Y" that is assumed to be present in excess in voltammetric cell. In Table 1 we give an overview of the definitions of major parameters used in theoretical calculations of considered mechanism. In this study, we utilized the MATHCAD 14 commercial software package to compute the theoretical voltammograms. It should be underlined that the reduction currents were defined as positive in the model, consistent with the US electrochemical convention.

3. RESULTS AND DISCUSSION

Numerous theoretical voltammetric models, designed to describe the electrochemical mechanisms of various redox proteins undergoing coupled chemical reactions, have already been utilized for cyclic and square-wave voltammetry at planar electrodes. Readers are encouraged to refer to some of those works for further information [6,10,11,12,16,18-28]. Although the inactivation of redox proteins is very often encountered in practice [1,2], only recently a theoretical voltammetric study in cyclic voltammetry that comprises chemical inactivation of initial redox form of lipophilic redox protein has been reported [29]. In this work, we report on SW voltammetric results that can apply to the irreversible inactivation of initial form of hydrophilic redox proteins and enzymes, but also to the irreversible inactivation of other redox systems. The primary outcomes of the investigated electrochemical mechanism, (described with Scheme 1), are presented by delineating the critical characteristics of the computed voltammetric curves. Moreover, a series of working curves are provided, which enable the determination of kinetic parameters pertinent to the rate of the chemical inactivation reaction associated with this mechanism To provide readers with insights into the distinctions between the current mechanism and its two most closely related mechanisms, this section of the work commences with brief explanations of some of the voltammetric characteristics of the $C_{rev}E$ and EC_{rev} mechanisms. Shown in Figure 1a-b are forward (reduction) and backward (reoxidation) curves of the square-wave voltammograms of electrode mechanisms coupled to reversible ("rev") preceding chemical reaction, the so-called $C_{rev}E$ mechanism (a) and with reversible follow-up chemical reaction or the so-called EC_{rev} mechanism (b). Voltammetric

curves in Figure 1 are calculated at magnitude of equilibrium constant of chemical steps (K_{eq} = 0.1), while they display the effect of dimensionless chemical parameter K_{chem}.

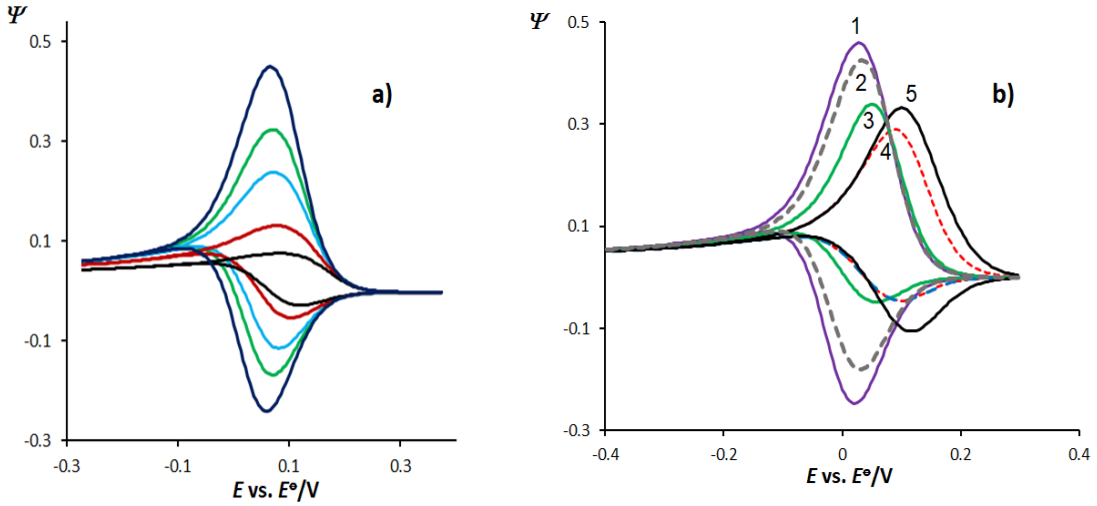

Figure 1. Effect of dimensionless chemical rate parameter K_{chem} to the features of forward (reduction) and backward (reoxidation) current components of square-wave voltammograms of diffusional CrevE (a) and ECrev (b) mechanisms. In both cases, rate of electron transfer step was K_{ET} = 5, while the constant of chemical equilibrium was set to K_{eq} = 0.1. In pattern (a), the dimensionless chemical rate parameter K_{chem} was set to 0.01; 0.5; 1; 2.5; 5 and 10 (from curve with lowest to the curve with highest current, respectively), while for the patterns (b) K_{chem} was set to 0.001 (1); 0.01 (2); 0.1 (3); 1 (4) and 10 (5). Other simulation conditions were: electron transfer coefficient α = 0.5, number of electrons exchanged n = 1, temperature T = 298 K, square-wave amplitude E_{sw} = 50 mV, potential step dE = 4 mV, frequency f = 10 Hz, diffusion coefficient D = 0.000005 cm^2s^{-1}.

As the rate of chemical reaction increases by the $C_{rev}E$ mechanism, one recognizes a stepwise evolution of "normal" voltammograms that converge to those of "simple" Ox + ne- ↔ Red systems [12] at large magnitudes of K_{chem} (see the curves with largest currents in figure 1a). At EC_{rev} mechanism, moderate chemical rates affect mainly the features of reoxidation (backward) voltammetric current components that get diminished in intensity (curves 2 and 3 in Figure 1b). In the EC_{rev} mechanism, the significant chemical reaction rates facilitate the rapid re-establishment of chemical equilibrium. As a result, the voltammograms exhibit nearly reversible characteristics that undergo a shift towards more positive potentials. (curves 4-5 in Figure 1b). The voltammograms depicted in Figure 1 can serve as a tool for gaining a better understanding of the disparities among $C_{rev}E$, EC_{rev}, and the electrode mechanism presented in this research. Figure 2 illustrates the impact of the dimensionless kinetic parameter associated with the electron transfer step (KET) on the characteristics of the forward-backward (a) and

net SW voltammetric curves of the electrode mechanism expounded upon in this study (Scheme I).

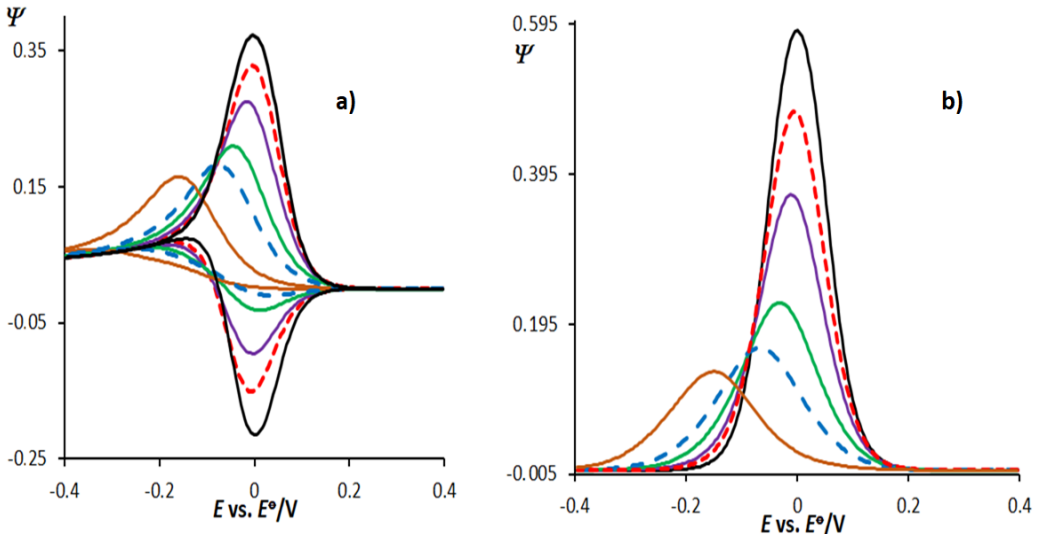

Figure 2. Effect of dimensionless rate parameter of electron transfer K_{ET} to the features of forward and backward (a) and net square-wave voltammograms of electrode mechanism considered in this work. Curves are calculated at negligible rate of chemical step (K_{chem} = 0.00001). K_{ET} was set to 3.0; 1.4; 0.35; 0.14; 0.07 and 0.014 by going from curve with highest toward curve with lowest peak currents in both (a) and (b), correspondingly. Other simulation conditions were same as those reported in Figure 1.

Voltammetric curves in Figure 2 are calculated at negligible rate of chemical reaction (K_{chem}=0.00001). In such scenario, decreasing of magnitude of K_{ET} leads to diminishing of all current components, while the position of the net SWV peaks shifts to more negative potentials. Obviously, curves in Figure 2 portray a well-known behavior of a simple Ox + ne- ↔ Red mechanism of water-soluble redox couple as a function of rate of electron transfer [12]. The features of voltammetric curves can undergo significant changes when the rate of the irreversible chemical step involving the initial reactant Ox is altered, even if the rate of the electron transfer step remains constant. As the chemical reaction irreversibly consumes the starting material of investigated redox protein, then it is reasonable to anticipate that augmenting the chemical rate will lead to a reduction in the current intensities of all SW voltammetric current components. Such an event is displayed in Figure 3 (see forward and backward curves in figure 3a, and corresponding net SWV components in Figure 3b). Under such circumstances, a fascinating topic for discussion is the impact of chemical reaction rates on the shapes of both forward and backward voltammetric curves in various regions of K_{chem}. Consistent with this mechanism, the intensities of both the forward and backward currents decrease with an increase in the rate of the chemical reaction. However, the backward current components retain their common peak-like shape even at very large magnitudes of K_{chem}, which

is visible in all reoxidation curves displayed in Figure 3a, and those given in the inset of that figure. Although the intensities of the currents associated with the reduction (forward) voltammetric curves decrease with an increase in K_{chem}, significant modifications in the shapes of the reduction curves are noticeable when they are calculated at higher rates of the chemical reaction. In region of $K_{chem} \geq 100$ (see curves in the inset of Figure 3a), an increase of rate of chemical reaction produces significant broadening of the reduction (forward) curves, which ultimately get shape of plateau rather than peak for magnitudes of $K_{chem} > 200$.

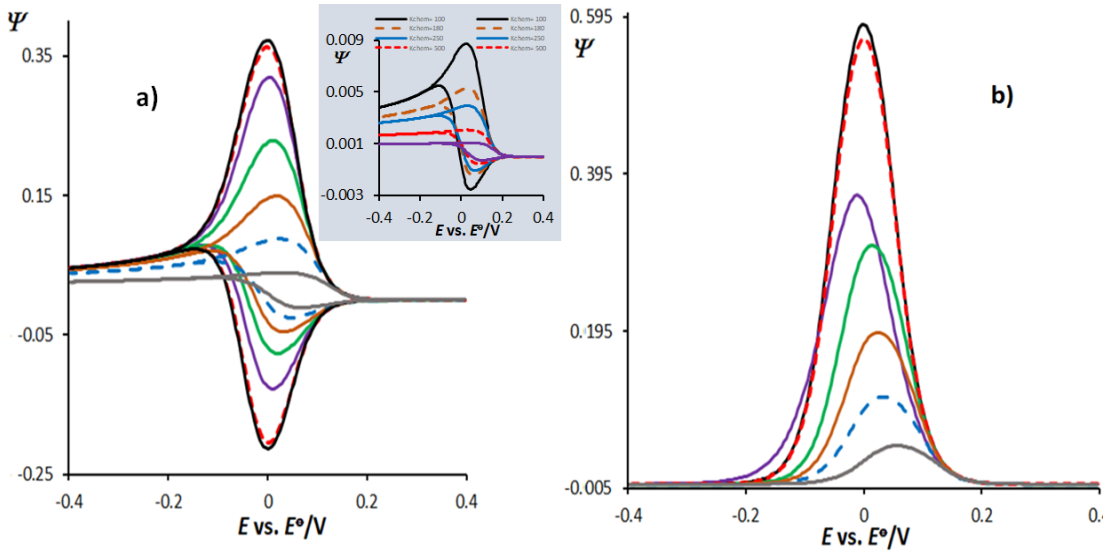

Figure 3. Effect of dimensionless chemical rate parameter K_{chem} to the features of forward (reduction) and backward (reoxidation) current components (a) and to net SW peaks (b) of square-wave voltammograms of electrochemical mechanism considered in this work. K_{chem} was set to 0.0001; 1.0; 10; 25; 50 and 100 (by going from curve with highest toward curve with lowest peak currents in both (a) and (b), respectively). Inset in pattern (a) displays forward and backward currents simulated at high rates of chemical reaction (simulated at $K_{chem} > 100$). K_{ET} was set to 3.0. Other simulation conditions were same as those reported in Figure 1.

The distinctive shapes of the reduction voltammetric currents arise primarily because the rate of the chemical reaction dominates over the rate of the electron transfer step. In general, the overwhelming permanent "consumption" of the initial electroactive material that happens in the time-frame of current-sampling segment of SW pulses leads to plateau-like forms of the reduction current components. At rates of chemical step described by $K_{chem} > 200$, the reduction voltammetric current components get a sort of sigmoidal shapes upon increasing the rate of chemical step. The behavior of voltammetric curves observed at high chemical reaction rates is reminiscent of that exhibited by the electrochemical-catalytic EC' mechanism when the regenerative reaction occurs at high rates [12,16]. The features observed at the curves of voltammetric patterns displayed in figure 3a are distinctive for this electrochemical mechanism

only, and they are not typical in voltammetry of other electrochemical mechanisms coupled with chemical reactions [12,16]. Hence, the characteristics of the voltammetric curves depicted in Figure 3, obtained at large rates of chemical step, can serve as a crucial indicator for identifying this particular electrode mechanism in SWV. Another indicative feature of the voltammograms displayed in figure 3 is the shift of the net SWV peaks towards more positive potentials as the rate of chemical step falls in the region $K_{chem} > 25$. Normally, this feature is associated to the electrode mechanisms that are linked with follow up chemical reactions coupled to the electrochemically generated product [12]. In this work, we have explored this characteristic of net SW voltammograms to construct working curves that are relevant to get access to the rate constant of chemical step.

Once the nature of the electrode mechanism elaborated in this work is evaluated, the second step is to develop a suitable methodology to determine the physical parameters related to the electron transfer step ($k_s^{\ominus}$, α), and that of the chemical reaction (k_c). Commonly, the "amplitude-based quasireversible maximum" approach [30] and some other "classical" methods described in [12,16] can be used for getting access to the values of $k_s^{\ominus}$ and α (experiments should be performed in absence of chemical reaction). One of rather specific attributes of considered electrode mechanism is the shift of position of net SWV peaks toward more positive potentials upon increasing of rate of chemical step (see the net SWV peaks in Figure 3b). Displayed in Figure 4a are the dependences between net SWV peak potentials ($E_{net,p}$) as a function of $\log(K_{chem})$.

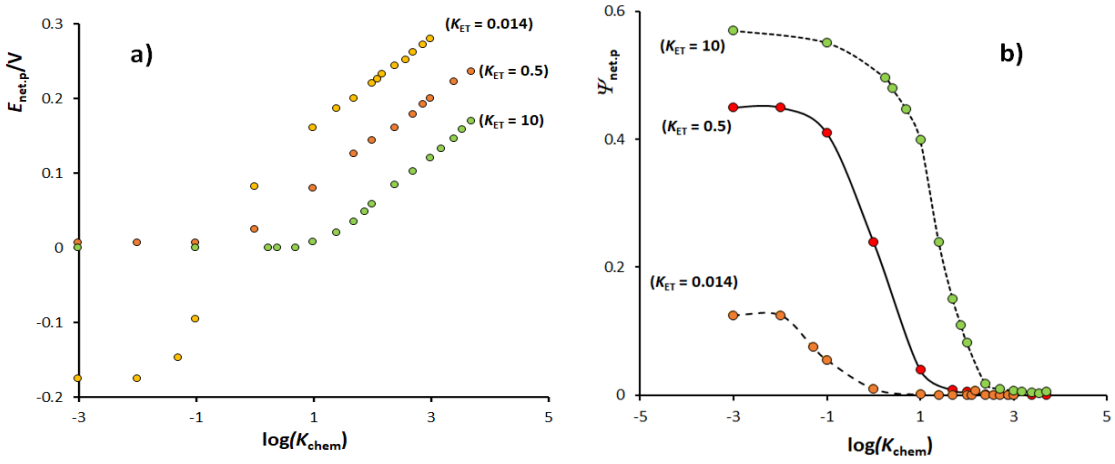

Figure 4. Dependences of the net SW peak potentials ($E_{net,p}$) (a) and net SW peak-currents (b) as a function of $\log(K_{chem})$, calculated at three different kinetics of electron transfer step. The magnitudes of the dimensionless kinetic parameter of electron transfer K_{ET} are given in the graphs. Other simulation conditions were same as those reported in Figure 1.

Note that the curves in figure 4a are constructed for three different magnitudes of K_{ET}. In all working curves presented in Figure 4a, linear parts at the dependences between $E_{net,p}$ and

log(K_{chem}) exist roughly in the regions 0.5 < log(K_{chem}) < 4.0. In these regions of chemical reaction rates, the slopes of the linear dependences of $E_{net,p}$ vs. log(K_{chem}) curves are almost identical and they have value of about +60 mV. The equations of the linear parts of curves displayed in figure 4a read: $E_{net,p}$ /V = 0.062 V x log(K_{chem}) - 0.086 V (for K_{ET} = 10); $E_{net,p}$/V = 0.06 V x log(K_{chem}) + 0.069 V (for K_{ET} = 0.5); and $E_{net,p}$ /V = 0.061 V x log(K_{chem}) + 0.09 V (for K_{ET} = 0.014). The last set of equations corresponding to the linear parts of $E_{net,p}$ *vs.* log(K_{chem}) dependences in Figure 4a can be explored for the determination of the rate constant of chemical inactivation reaction, if the magnitude of K_{ET} is determined previously. At this stage it is worth to mention that sigmoidal dependences also exist between the net SWV peak currents $\Psi_{net,p}$ and log(K_{chem}) (see Figure 4b). For constant electron transfer coefficient and constant temperature, the slopes of linear parts of the working curves presented in figure 4b are function of the magnitude of K_{ET}. The linear parts of the curves displayed in Figure 4b can be explored as an alternative tool to get access to magnitude of K_{chem}, if magnitudes $k_s^{\ominus}$ and that of electron transfer coefficient are previously determined.

4. CONCLUSION

Despite the great progress of voltammetric theories performed to describe various electrochemical mechanisms in last 30 years, there are still important mechanisms yet to be elaborated theoretically. As the processes of irreversible inactivation often happen important enzymatic systems such as glutathione peroxidase, tyrosine phosphatases, cysteine cathepins and many more [31-34], we present in this work a series of theoretical results related to the SW voltammetric behavior of hydrophilic redox enzymes and proteins, whose initial form is simultaneously engaged in an electrode transformation and in parallel irreversible chemical transformation (irreversible inactivation). By exploring the voltammetric outputs of this model under conditions of square-wave voltammetry, we present the readers a set of representative voltammetric curves that can help in evaluating the nature of this important electrochemical mechanism. A systematic review of features of reduction and oxidation curves of this mechanism, studied as a function of electron transfer rate and the rate of irreversible chemical step, is summarized in Table 2. The voltammetric curves displayed in Table 2 are specific for this electrochemical mechanism, and by exploring their features one can distinguish the current mechanism from other electrochemical systems in which electron transfer step is coupled with preceding, regenerative or follow up chemical reactions. In addition, with the hints given in figures 3 and 4 in previous section, one can develop a suitable voltammetric methodology to get access to rate constant of chemical inactivation. With the initial results of this work, we hope that a platform will be created for pursuing novel theoretical studies on inactivation processes of hydrophilic redox proteins in square-wave voltammetry.

When performing experiments with systems that are previously known to obey this electrode mechanism, it is important to make synchronization of adding substrate “Y” in

electrochemical cell with the initiation of voltammetric measurements. This is because the chemical reaction also takes place even in conditions of open circuit. From technical point of view, by working with classical electrochemical cell, it will be a challenging task to make experiments in which the chemical reaction of inactivation will be synchronized with the time of applying the bias. This is especially demanding task for systems characterized with large rates of chemical reactions. One possible technical solution to overcome this problem is to work with flow voltammetric cells. Other possibility is to use some of novel potentiostats with flow voltammetric cells, where sequential range of frequencies can be applied during a single experiment. Although the open circuit experiments in this mechanism are an important segment from technical point of view, it is worth to underline that their contribution is seen only as a starting point in the real experiments and in the theoretical calculations. Regardless of what is the rate of inactivation reaction taking place under open circuit, in reality what we detect is always the magnitude of current-potential changes that are measured versus that initial point. Same discussion holds for all other electrochemical mechanisms coupled with chemical reactions as elaborated in [12].

Table 2. Reduction (forward) and oxidation (backward) current components of the square-wave voltammograms simulated at different rates of electron transfer step and at different kinetics of irreversible chemical reaction. For all curves presented in this table, a square-wave amplitude of 50 mV and potential step of 4 mV were used. The electron transfer coefficient in all simulations was set to $\alpha = 0.5$. Other simulation conditions were same as in Figure 1.

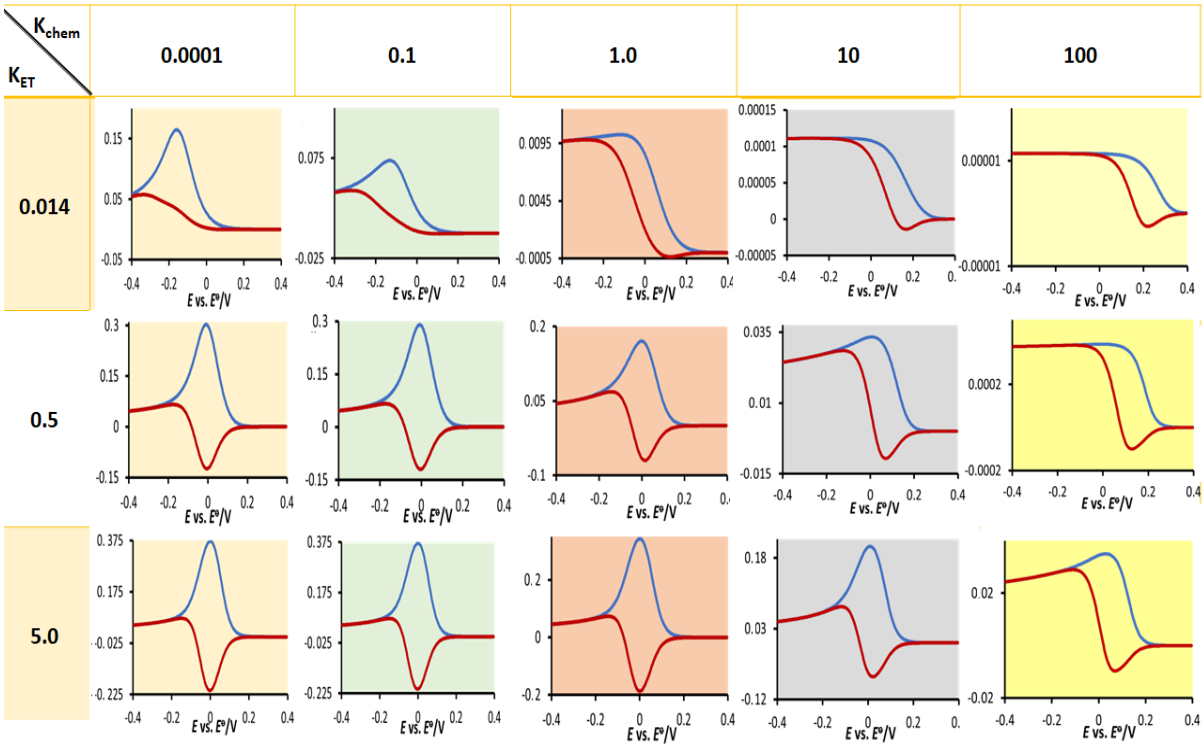

Acknowledgments

Rubin Gulaboski would like to thank Alexander von Humboldt Foundation for support in 2021 during research stay at the University of Göttingen, Germany.

Declarations of interest

The authors of this work declare that this research was conducted in absence of any commercial or financial relationships that could be considered as a potential conflict of interest.

REFERENCES

[1] D. Gamenara, G. A. Seoane, P. Saenz-Méndez and P. Domínguez de María, Redox biocatalysis: Fundamentals and applications, John Wiley & Sons (2013).

[2] A. Van Loey, Indrawati, C. Smout and M. Hendrickx, Inactivation of enzymes: from experimental design to kinetic modeling, in Handbook of food enzymology (J. R. Whitaker, A. G. J. Voragen, W. S. Dominic, eds.), CRC Press, New York (2002).

[3] S. Adcock, and J. A. McCommon, Chem. Rev. 106 (2006) 1589.

[4] F. A. Armstrong, Applications of voltammetric methods for probing the chemistry of redox proteins In: Bioelectrochemistry: Principles and practice (Lenaz G, Milazz G, eds), Birkhauser Verlag AG, Basel (1997).

[5] L. P. Jenner, and J. N. Butt, Curr. Opin. Electrochem. 8 (2018) 81.

[6] C. Legler, and P. Bertrand, Chem. Rev. 108 (2008) 2379.

[7] J. Hirst, Biochim. Biophys. Acta Bioener. 1757 (2006) 225.

[8] V. Fourmond, and C. Leger, An introduction to electrochemical methods for the functional analysis of metalloproteins, in Practical approaches to biological inorganic chemistry (R. R. Crichton and R. O. Louro, eds.), Elsevier (2020).

[9] K. A. Vincent, A. Parkin, and F. A. Armstrong, Chem. Rev. 107 (2007) 4366.

[10] R. Gulaboski, P. Kokoskarova, and S. Mitrev, Electrochim. Acta 69 (2012) 86.

[11] F. A. Arsmstrong, Electrifying metalloenzymes in: Metalloproteins: Theory, calculations and experiments (Cho AE, Goddar WA III, eds), CRC Press, Taylor&Francis Group, London, New York (2015).

[12] V. Mirceski, S. Komorsky-Lovric, and M. Lovric, Square-wave voltammetry: Theory and application (F. Scholz, Ed.), Springer, Berlin (2007).

[13] R. Gulaboski, V. Mirceski, I. Bogeski, and M. Hoth, J. Solid State Electrochem. 16 (2012) 2315.

[14] R. Gulaboski, V. Mirceski, and M. Lovric, J. Solid State Electrochem. 23 (2019) 2493.

[15] V. Mirceski, R. Gulaboski, M. Lovric, I. Bogeski, and M. Hoth, Electroanalysis 25 (2013) 2411.

[16] A. Molina and J. Gonzales, Pulse voltammetry in physical electrochemistry and electroanalysis, in Monographs in electrochemistry (F. Scholz, ed.), Springer, Berlin Heidelberg (2016).
[17] M. L. Olmstead, R. G. Hamilton, and R. S. Nicholson, Anal. Chem. 41 (1969) 260.
[18] M. Lopez-Tenes, J. Gonzalez, and A. Molina, J. Phys. Chem. C 118 (2014) 12312.
[19] H. N. Zhang, Z. Y. Guo, and P. P. Gai, Chinese J. Anal. Chem. 37 (2009) 461.
[20] J. Gonzalez, M. Lopez-Tenes, and A. Molina, J. Phys. Chem. C 117 (2013) 5208.
[21] M. A. Mann, and L. A. Bottomley, Langmuir 31 (2015) 9511.
[22] G. P. Stevenson, C.-Y. Lee, G. F. Kennedy, A. Parkin, R. E. Baker, K. Gillow and F A. Armstrong, D. J. Gavaghan, and A. M. Bond, Langmuir 28 (2012) 9864.
[23] V. Fourmond, E. S. Wiedner, W. J. Shaw, and Ch. Léger, J. Am. Chem. Soc. 141 (2019) 11269.
[24] J. González, and J.A. Sequí, ChemCatChem. 13 (2021) 747.
[25] V. Mirceski, D. Guziejewski, and R. Gulaboski, Anal. Chem. 91 (2019) 14904.
[26] C. Léger, S. J. Elliott, K. R. Hoke, L. J. C. Jeuken, A. K. Jones, and F. A. Armstrong, Biochemistry 42 (2003) 8653-8662.
[27] M. Janeva, P. Kokoskarova, V. Maksimova, and R. Gulaboski, Electroanalysis 31 (2019) 2488.
[28] J. R. Winkler, and H. B. Gray, J. Am. Chem. Soc. 136 (2014) 2930.
[29] R. Gulaboski, Monatsh. Chem. 154 (2023) 141
[30] D. Guziejewski, V. Mirceski, and D. Jadresko, Electroanalysis 27 (2015) 67.
[31] R. R. Ramsey, L. Basile, A. Maniquet, S. Hagenow, M. Pappalardo, M. C. Saija, S. D. Bryant, A. Albrecht, and S. Guccione, Molecules 25 (2020) 5908.
[32] J. M. Strelow, SLAS Discovery 22 (2017) 3.
[33] C-S. Cho, S. Lee, G. T. Lee, H. A. Woo, E-J. Choi, and S. G. Rhee, Antiox. Redox Signal. 12 (2010).
[34] B. Mirkovic, I. Sosic, S. Gobec, J. Kos, Plos One 6 (2011) e27197.